Characterization of relaxation processes in interacting vortex matter through a time-dependent correlation length

Michel Pleimling and Uwe C. Täuber

Department of Physics, Virginia Tech, Blacksburg, VA 24061-0435, USA

Abstract. Vortex lines in type-II superconductors display complicated relaxation processes due to the intricate competition between their mutual repulsive interactions and pinning to attractive point or extended defects. We perform extensive Monte Carlo simulations for an interacting elastic line model with either point-like or columnar pinning centers. From measurements of the space- and time-dependent height-height correlation function for lateral flux line fluctuations, we extract a characteristic correlation length that we use to investigate different non-equilibrium relaxation regimes. The specific time dependence of this correlation length for different disorder configurations displays characteristic features that provide a novel diagnostic tool to distinguish between point-like pinning centers and extended columnar defects.

1. Introduction

The characterization and optimization of the properties of vortex matter in disordered type-II superconductors has been a prominent research focus in condensed matter physics over the past two decades [1, 2]. Detailed experimental and theoretical studies of interacting magnetic flux lines subject to different types of attractive pinning centers have yielded rich equilibrium phase diagrams with novel glassy states as well as an intriguing complexity in the associated dynamical phenomena. The mean-field Abrikosov flux lattice in pure type-II superconductors is already destroyed at low temperatures by point-like defects and replaced by a disorder-dominated vortex glass phase, wherein the vortices are collectively pinned, and display neither translational nor orientational long-range order [3, 4, 5, 6]. Firm theoretical arguments furthermore support the existence of a topologically ordered dislocation-free Bragg glass phase at low magnetic fields or sufficiently weak disorder [7, 8, 9, 10, 11, 2]. Extended attractive defects such as columnar pins localize the flux lines in their vicinity; the resulting low-temperature Bose glass phase is distinguished from the vortex or Bragg glass through its infinite tilt modulus or vanishing linear response to a magnetic field rotation (transverse Meissner effect) [12, 13, 14, 15]. It is important to note that transverse flux line fluctuations become strongly suppressed in the Bose glass, in stark contrast to the disorder-induced line roughening in the presence of randomly distributed point pinning centers.

The quite distinct flux line fluctuation spectra that result for various pinning centers should naturally be observable in non-equilibrium relaxation processes, wherein the vortex system slowly approaches a low-temperature equilibrium glassy state after being initialized in a very different configuration. Observing these relaxation features could thus provide an effective characterization tool for type-II superconducting samples. Previous numerical studies of the relaxation processes that take place in the glassy phases of vortex matter focused on a variety of one- and two-time quantities, as for example the radius of gyration, the two-time vortex line height-height autocorrelation function, or the two-times vortex line roughness, to name but a few [16, 17, 18, 19, 20, 21, 22]. From these investigations the following coherent picture is emerging.

First, one notes that the non-equilibrium properties deep inside the glassy phase are very different if both attractive and repulsive defects are considered [16, 17] or if only attractive pinning centers are present [20, 21, 22]. For vortices in type-II superconductors, however, material defects are exclusively attractive, thus providing a pinning landscape with deep wells in an otherwise flat potential. This is the case that we consider in this paper.

Second, relaxation processes for vortex matter in type-II superconductors are in general dominated by two strongly competing effects: the pinning of the flux lines due to attractive defects and the repulsive interaction between vortices. In the presence of thermal fluctuations various subtle crossover scenarios are encountered. For example, for defects of intermediate strength a two-step relaxation, reminiscent of that observed in structural glasses, is revealed in the two-time height-height autocorrelation function [20, 21, 22]. Furthermore, the flux line relaxation characteristics are found to markedly depend on the type of disorder present in the sample [21, 22], and quite complex non-universal features emerge that vary with intrinsic material as well as external control parameters such as the temperature and the external magnetic field that sets the overall vortex density.

Important insights into relaxation properties of systems with slow dynamics can also be gained from the investigation of time- and space-dependent correlation functions and from the time dependence of characteristic growing length scales derived from these quantities; see Refs. [25, 26, 27, 28, 29, 30, 31, 32, 33] for various recent examples. In Refs. [34, 35] the time-dependent length scale for a two-dimensional array of vortices in the presence of weak point-like disorder was calculated analytically and the resulting aging properties were studied. In this present work, we employ extensive Monte Carlo simulations to investigate non-equilibrium relaxation processes for interacting flux lines in disordered type-II superconductors through a time-dependent characteristic length distilled from the space-time transverse vortex height-height correlation function. Using an effective description of the vortices as thin fluctuating elastic lines, valid in the extreme London limit and low flux density, we study systematically how the different contributions to the Hamiltonian affect this growing correlation length in distinct temporal regimes. We specifically compare two different types of attractive pinning centers, namely randomly distributed point-like disorder and correlated columnar defects, and identify typical signatures in the associated correlation lengths for these different material defect classes, as the vortex system equilibrates towards the disorder-dominated Bragg or Bose glass phase, respectively.

The paper is organized in the following way: In the next Section we recall the effective Hamiltonian pertaining to the elastic line description of interacting magnetic vortices and discuss the model parameters used in our numerical simulations. We then introduce the space- and time-dependent transverse height-height correlation function and the time-dependent characteristic length derived from that quantity. Section III contains our results, both for point-like as well as for correlated defects. We conclude in Section IV with a brief summary and outlook.

2. Model and observables

In our study we consider three-dimensional vortex systems composed of N interacting flux lines. In the extreme London limit, where the superconducting coherence length is assumed much smaller than the London penetration depth, vortex lines in type-II superconductors are well described by a coarse-grained elastic line model [14]. Introducing the trajectory $\mathbf{r}_j(z) = x_j(z)\hat{\mathbf{x}} + y_j(z)\hat{\mathbf{y}}$ of flux line j, where z represents the coordinate in the direction of the applied magnetic field perpendicular to the xy plane, the effective Hamiltonian for a sample of thickness L is given by

$$H_N = \frac{\tilde{\epsilon}_1}{2} \sum_{j=1}^{N} \int_0^L \left| \frac{d\mathbf{r}_j(z)}{dz} \right|^2 dz + \sum_{j=1}^{N} \int_0^L V_D\big(\mathbf{r}_j(z)\big) \, dz$$
$$+ \frac{1}{2} \sum_{i \neq j} \int_0^L V\big(|\mathbf{r}_i(z) - \mathbf{r}_j(z)|\big) \, dz \ . \tag{1}$$

The first term here describes the elastic line tension, with the tilt modulus $\tilde{\epsilon}_1 = 0.18 \, \epsilon_0$ for YBCO, where $\epsilon_0 = (\phi_0/4\pi\lambda_{ab})^2$, with the magnetic flux quantum $\phi_0 = hc/2e$ and the London penetration depth λ_{ab}, sets the interaction energy scale. Using for our simulation parameter values typical for YBCO, we take $\lambda_{ab} = 34 \, b_0$ with $b_0 = 35$ Å and thus $\epsilon_0 \approx 1.9 \times 10^{-6}$ erg/cm [1]. The second contribution in (1) captures the disorder-induced attractive potential due to localized pinning centers, which we model as potential wells with in-plane radius b_0 and depth $U_0 = p \, \epsilon_0$,

with the strength parameter p varying between 0 and 0.20. The third term finally represents the repulsive vortex-vortex pair interaction. Consistent with the extreme London limit, this repulsion is purely in-plane between flux line elements and given by $V(r) = 2\epsilon_0 K_0(r/\lambda_{ab})$, where K_0 denotes the zeroth-order modified Bessel function. As $V(r)$ decreases exponentially for $r \gg \lambda_{ab}$, we truncate this vortex interaction at half of the lateral system size [20].

Using a discretized version of the Hamiltonian (1) and periodic boundary conditions, we perform standard Metropolis Monte Carlo simulations [23, 24] at temperature $T = 10$ K, corresponding to $k_B T/b_0 \epsilon_0 \approx 0.002$. This temperature choice assures that the system resides deep in a disorder-dominated glassy regime, namely most likely the Bragg glass phase for the case of point pinning centers, and the Bose glass for extended columnar pins [20]. Spatial discretization is done in the z direction in such a way that we have L equidistant layers separated by the basic microscopic distance scale b_0. Our system contains $N = 16$ vortices, with the number of flux line elements per vortex ranging from $L = 640$ to $L = 2560$. The in-plane dimensions are set to $L_x = \frac{2}{\sqrt{3}} \times 8\lambda_{ab}$ and $L_y = 8\lambda_{ab}$, and we checked that the vortices arrange in a triangular Abrikosov flux lattice in the absence of disorder. In each layer, we place $N_D = 1116$ pinning centers. For the case of random point defects, these pinning centers are randomly distributed and chosen independently for each layer. For columnar defects aligned parallel to the magnetic field along the z direction, we instead repeat the same spatial distribution pattern for each layer. As usual, we define as a Monte Carlo time step a consecutive series of NL updates; *i.e.*, on average every flux line element is updated once during each Monte Carlo time step. In the following, all distances and length scales are measured in units of b_0, and time in terms of Monte Carlo steps.

In order to study the build-up of spatial correlations, we prepare an out-of-equilibrium initial state by randomly placing straight lines, oriented along the z direction, in the system. While this initial configuration is well-suited for our investigation, it is not a state that can be set up easily in experiments. Initial out-of-equilibrium conditions closer to experimentally realizable situations can be achieved through temperature or field quenches, as discussed recently in Ref. [22].

After having prepared the system in this initial state, we bring the system in contact with a heat bath at temperature $T = 10$ K and follow its subsequent time evolution by measuring the space- and time-dependent height-height correlation function for lateral flux line displacements,

$$C(r,t) = \frac{1}{2}\big[C_x(r,t) + C_y(r,t)\big] \,, \tag{2}$$

with

$$C_x(r,t) = \Big\langle \big[x_j(z,t) - \overline{x}_j(t)\big]\big[x_j(z+r,t) - \overline{x}_j(t)\big]\Big\rangle \,, \tag{3}$$

and similarly for $C_y(r,t)$. Here $x_j(z,t)$ is the x coordinate of the flux line element z of line j at time t, whereas $\overline{x}_j(t)$ represents the mean x position of line j. The height-height correlation results from a fourfold average: an average over all NL vortex elements, over several noise realizations, over different initial configurations, and over independent disorder realizations. The data discussed in the following result from averaging over typically 40 independent runs for non-interacting vortex lines, whereas for interacting lines we averaged over at least 400 different runs.

A time-dependent correlation length $\xi(t)$ can be extracted from the height-height correlation function (2) by imposing the condition that for a fixed value of t the

correlation function $C(r,t)$ has decreased by a factor C_0 from its maximum value $C(0,t)$:

$$C\big(\xi(t),t\big)/C(0,t) = C_0 \ . \tag{4}$$

We have used $C_0 = 0.5$ in the following, but have verified that the temporal evolution of the characteristic length $\xi(t)$ is qualitatively unchanged when a different value is chosen. An alternative length scale can be obtained from integral estimators [36]. Comparing these two approaches we did not find any significant qualitative differences.
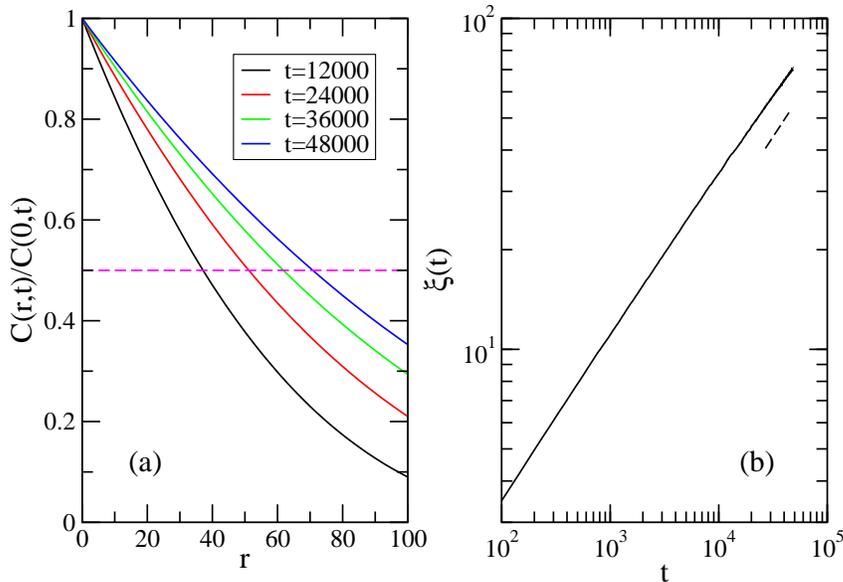

Figure 1. (a) Normalized space-time height-height correlation function $C(r,t)/C(0,t)$ for free flux lines with $L = 2560$ as a function of distance r for four different times. The intersections with the dashed magenta line $C_0 = 0.5$ yield a time-dependent characteristic length. (b) Time-dependent correlation length $\xi(t)$ obtained from $C(r,t)$. The dashed line indicates the expected slope $1/2$ for free diffusive motion.

Fig. 1 shows the space-time height-height correlation function (a) and the derived characteristic length $\xi(t)$ (b) for the case of free lines (*i.e.*, non-interacting vortices in the absence of any disorder). As expected for this simple case, free lines undergo purely diffusive transverse motion, resulting in a square-root increase with time of the dynamic length scale, as indicated by the dashed line in Fig. 1(b). The free-line data will serve as baseline in the next Section when we turn to the effects of the different contributions in the Hamiltonian on the growing length scale $\xi(t)$.

3. Results

In the following discussion of our Monte Carlo simulation data, we first focus on samples with point-like defects, before considering later systems with columnar pinning centers. As we will see, these different defect types reveal themselves through distinct characteristic features in the time-dependent correlation length.

3.1. Point defects

Point-like pinning sites are localized crystal defects, as for example oxygen vacancies in ceramic superconductors, that may occur naturally or can be introduced artificially. Irrespective of their origin, they exert a short-range attractive force on the magnetic flux lines. These pinning sites are normally located at random positions in the sample. However, point-like defects can also be distributed in non-random ways; *e.g.,* recent intriguing studies have investigated the enhanced pinning efficiency of conformal pinning arrays [37, 38, 39].

Figure 2 summarizes our findings for randomly placed attractive pinning sites. First, we consider in Fig. 2(a) the simplified case of non-interacting flux lines in a random pinning landscape, before we turn to the full problem of a thermal system of interacting magnetic vortices in a three-dimensional space with point pinning centers in Fig. 2(b).

For non-interacting vortices in a disorder-free environment, the displacement components of a flux line element in the plane perpendicular to the z direction satisfy the Edwards-Wilkinson (or stochastic diffusion) equation. Consequently, the correlation length obtained from the space-time height-height correlation function for lateral line fluctuations (2) increases with time as $\xi(t) \sim t^{1/2}$, see Fig. 1(b). The introduction of pinning centers constrains the transverse vortex fluctuations, as some flux line elements are trapped at favorable near-by attractive pinning sites. This trapping can be temporary and transient for weak pinning strengths, where thermal noise is strong enough to allow the escape from the potential wells, or become permanent for strong pinning centers. These different situations are clearly reflected in a change of the behavior of $\xi(t)$ when increasing the pinning stength p, as demonstrated in Fig. 2(a). Inspection of the graphs reveals that the correlation length grows diffusively at early times, just like that of a free line. The randomly placed straight vortices first need to roughen thermally and then explore their disordered environment before a sizeable number of flux line elements reaches close enough to pinning sites to become trapped. Once they are captured, lateral flux line fluctuations are impeded, and hence the correlation length increase is slowed down when compared to the behavior of a free line. As one would expect, the crossover time at which deviations from the free-line behavior are observed decreases noticeably with increasing pinning strengths p. For weak strengths, *c.f.* the data for $p = 0.01$ and $p = 0.02$ in Fig. 2(a), the correlation length maintains an algebraic temporal behavior $\xi(t) \sim t^{1/z}$ in the long-time limit, yet with a dynamic scaling exponent $z > 2$. Thus for $p = 0.01$ we obtain the value $1/z \approx 0.15$, whereas for $p = 0.02$ we measure $1/z \approx 0.09$. For stronger pinning strengths, *e.g.*, $p = 0.05$ and $p = 0.20$, $\xi(t)$ becomes effectively independent of the value of p, and stops increasing after around 10^4 Monte Carlo time steps. For such strong point pinning centers, the vortices are permanently trapped for the duration of our simulation, and different flux line segments remain largely uncorrelated. Closer inspection of $\xi(t)$ for large p, depicted in the inset of Fig. 2(a), reveals even a slight decrease of $\xi(t)$ for large t as additional flux line elements are captured by the point defects, thus further reducing the lateral vortex fluctuations. We remark that we have observed qualitatively similar behavior both for the flux line mean-square displacement and radius of gyration in Langevin molecular dynamics simulations, see Fig. 5 in Ref. [21].

Additional interesting features emerge in our simulations of the full problem of interacting vortex lines in a pinning landscape with attractive point defects. As shown
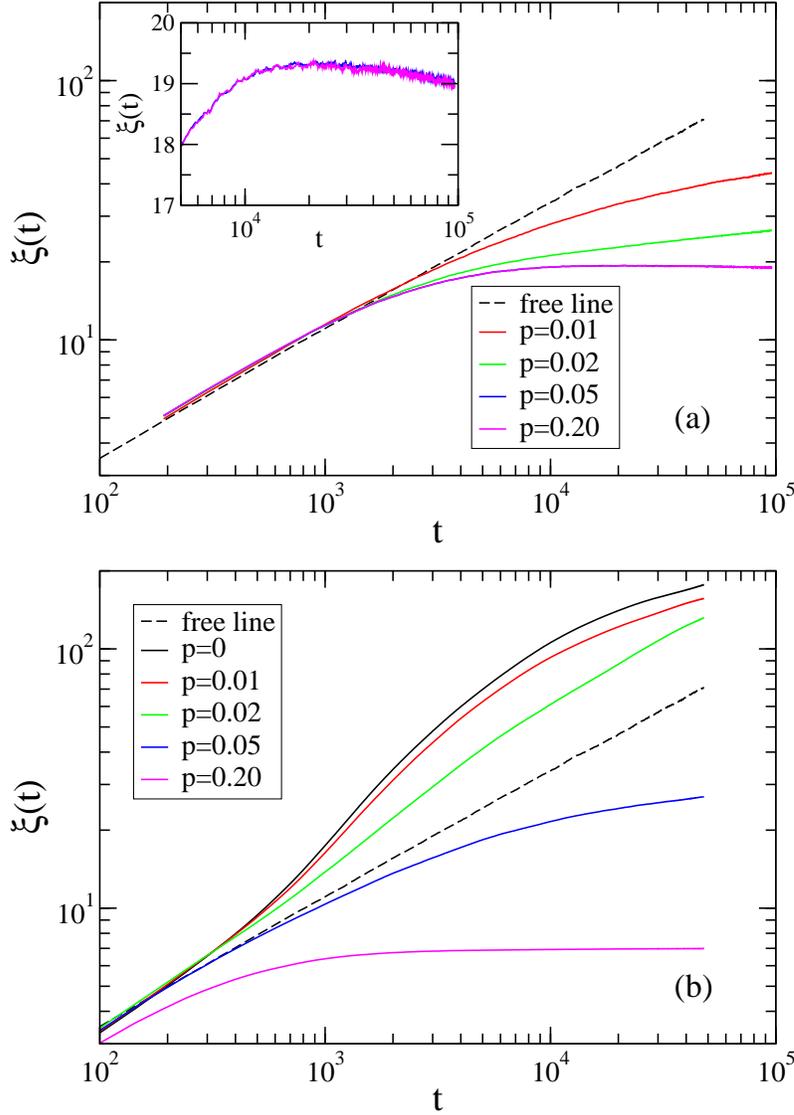
Figure 2. Correlation length $\xi(t)$ derived from the space-time height-height correlation function (4) in the presence of point-like pinning centers for vortex lines of length $L = 2560$: Figure (a) shows the time evolution for non-interacting flux lines, whereas the correlation lengths for interacting vortices are shown in (b). The inset in (a) focuses on the long-time behavior of non-interacting lines in the presence of strong pins. In both figures the dashed line represents the correlation length of a free line, *c.f.* Fig 1(b).

in Fig. 2(b), marked differences between weak and strong pins are again revealed by the correlation length $\xi(t)$. For weak pinning strengths three different regimes can be observed. At very early times the vortices still behave essentially like free lines, and the transverse correlations along the lines are not yet affected by the mutual repulsive vortex interactions or the pinning to localized defect sites. This early-time

regime, however, is very short, as it lasts only a few hundred Monte Carlo time steps. After that the flux lines start rearranging themselves, build up longer-range spatial correlations, and tend to form a triangular lattice, which is revealed by enhanced values of $\xi(t)$ when compared to the characteristic length scale of the free line. The full black line in Fig. 2(b), which refers to the situation without pins, clearly indicates the temporal changes of the correlation length when the Abrikosov flux lattice becomes established. Adding weak pins, as for example for $p = 0.01$ (red line in the figure) does not have a major impact on the correlations as the relatively strong vortex-vortex interactions prevent efficient pinning of flux line elements. Upon further increasing the pinning strength, the flux line interactions lose against the attractive point disorder, and more and more flux line elements get trapped. This induces a slowing down of the growth of $\xi(t)$ and, ultimately, a termination of the further increase of this characteristic length. Note that for the largest values of p employed in our simulations, the ultimate correlation length for interacting vortices is much smaller than for non-interacting flux lines, compare the case $p = 0.20$ in Fig. 2(a) and Fig. 2(b). In fact, flux lines are quickly pushed away from their random initial locations due to their repulsion from the other vortices, and thus faster reach favorable pinning centers from which they cannot escape within the simulation time window. We again note that similar temporal ranges are observed for strong point defects in Langevin molecular dynamics simulation data for the mean-square displacement and gyration radius of mutually repelling flux lines, *c.f.* Fig. 9 in Ref. [21]; yet it is also important to realize that the detailed crossover times separating the distinct dynamical regimes do depend on the precise observable under investigation.

3.2. Columnar defects

As for point-like disorder, correlated columnar defects can appear naturally in a superconductor sample or can result from tailored manipulations of the sample. Line dislocations provide an example of naturally occurring linearly extended defects of this type. High-energy ion radiation yields material damage tracks used to pin vortex lines in type-II superconductors; alternatively, linear pinning centers, even with pre-arranged spatial distribution, can be engineered during material growth. Columnar defects are known to provide a much more efficient pinning mechanism for flux lines than uncorrelated point disorder [40, 1].

In our comparative study of point-like and columnar pinning centers, we distribute the same number of pinning sites per layer; the crucial difference is that for columnar defects this pattern repeats itself from layer to layer. It follows that in the presence of columnar pins, flux lines are much less likely to encounter a randomly placed defect. One therefore expects an average behavior much closer to that of vortices moving in a disorder-free environment. Yet on the other hand, once a vortex segment is captured by an extended pinning site that is correlated across the sample layers, there is a high probability that the whole flux line will become trapped [21]. Such vortices that are localized at a linear defect along their entire length hardly ever escape this extended pinning potential.

The time-dependent correlation length displayed in Fig. 3 reflects both the behavior of a free vortex at early times and the pinning of whole lines to columnar defects at later times. Let us first focus on the case of non-interacting vortices shown in Fig. 3(a). We observe that in the absence of mutual repulsion between the flux lines, the behavior of the characteristic length $\xi(t)$ is independent of the pinning
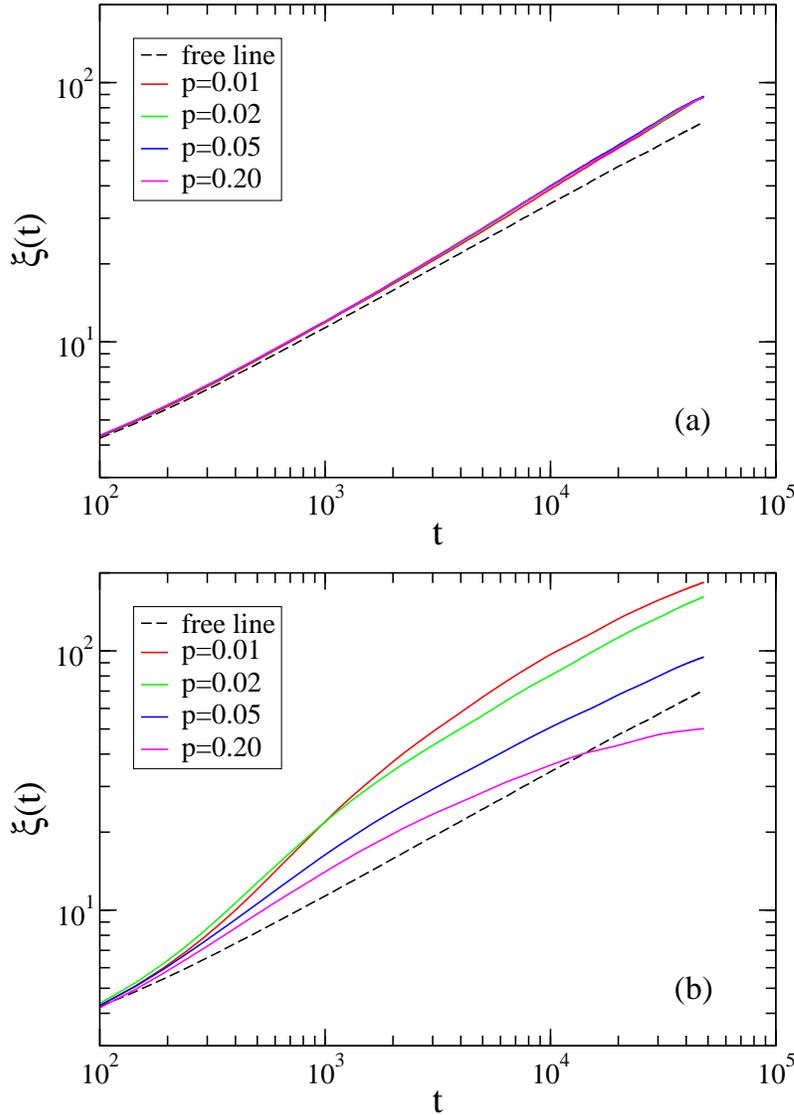
Figure 3. Time-dependent correlation length $\xi(t)$ in the presence of columnar defects. Figure (a) shows the time evolution for non-interacting vortices, whereas in (b) the correlation lengths for interacting flux lines are shown. In both figures the dashed line represents the correlation length of a free line. The vortex lines are composed of $L = 2560$ elements.

strength. This apparent universal feature is of course due to the fact that a vortex captured by an extended columnar pin cannot escape from this trap but instead remains firmly localized at the defect. We also note that the correlation length in a system with extended defects only displays rather small deviations from the free-line behavior. This is readily understood by remembering that the features revealed in $\xi(t)$ result from superposition of the height-height correlations of lines that have remained free, *i.e.*, not captured by defects, and of vortices trapped by columnar

pins whose transverse fluctuations are much suppressed. At first look it might be puzzling that the correlation length in systems with defect lines is slightly *larger* than for the free vortices. This behavior is explained by the observation that different segments of very long flux lines can be caught by spatially separated columnar defects. These captured parts are connected by segments with high elastic energy and strong correlations between the flux line elements. In order to check this interpretation we also ran simulations for much shorter vortex lines (comparable to those studied in Ref. [21]) where it is unlikely that the vortices are caught by more than one line defect. As expected, the correlation length for these smaller lines is always below that measured for free lines.

The situation becomes considerably more complicated for the full problem of interacting vortex lines subject to columnar pinning centers. We infer from Fig. 3(b) for small pinning strengths p a behavior for $\xi(t)$ that is qualitatively similar to that encountered for point-like defects: Due to their mutual repulsion, the vortices are displaced from their initial positions and tend to form an Abrikosov lattice, a process only slightly impeded by the randomly placed columnar defects in the system. For stronger defects, one essentially observes again the superposition and mixing of two different types of behavior, namely that of hitherto unbound lines that try to arrange themselves at least locally in a triangular lattice, and the features of lines that have already become trapped by defect columns and display reduced lateral fluctuations. However, in contrast to the data for non-interacting lines shown in Fig. 3(a), these two subsets of flux lines are not completely independent, since their dynamics and correlations become connected through the vortex-vortex interactions. As a result, the correlation length $\xi(t)$ keeps increasing with time, even for pinning strengths for which in samples with point-like defects we observed rapid saturation, compare Fig. 2(b) with Fig. 3(b) for the case $p = 0.20$. This behavior differs from that of the gyration radius that changes non-monotonically with time, but is similar to the time-dependence of the flux line mean-square displacement [21].

4. Conclusion

Vortices in type-II superconductors display very complex non-equilibrium properties, owing to the competition between different but comparable energy scales: elastic flux line tension, mutual vortex repulsion, defect pinning, and thermal noise. Using extensive Metropolis Monte Carlo simulations for an effective elastic line model with realistic parameters for YBCO, we aimed at investigating the non-equilibrium relaxation processes in this system through extracting a time-dependent correlation length $\xi(t)$ from the space-time lateral flux line height-height correlation function. We found that this characteristic length displays very rich behavior that allows us to identify different temporal relaxation regimes. Moreover we observe markedly different time dependences for point-like and extended columnar attractive defects that originate from the quite distinct underlying fluctuation spectra.

In previous studies of the relaxation kinetics of vortex matter in disordered type-II superconductors [16, 17, 18, 19, 20, 21, 22], various single-time quantities and two-time correlation functions, for example the two-time height-height autocorrelation function, the two-time mean-square displacement, and the two-time vortex density-density autocorrelation function, have been measured. Two-time quantities often yield important insights into relaxation processes far from equilibrium, but the physical interpretation of their behavior can also be quite challenging. The correlation length

studied in this work has the virtue of being simple and its signatures comparatively easy to understand. In addition, its characteristic features yield insights into different temporal relaxation regimes and into the emerging distinctions between uncorrelated point pins and extended linear defects.

Time-dependent correlation lengths have been the focus of several recent numerical investigations that probed non-equilibrium relaxation processes in disordered systems [28, 29, 30, 31, 32, 33]. However, most of these studies dealt with rather simple models as, *e.g.*, disordered Ising systems. Our work reveals that a time-dependent length scale can also be extracted for much more complex situations exemplified here by vortex matter subject to thermal fluctuations, disorder, and long-range interactions. In disordered ferromagnets, the relevant growing length scale $L(t)$ obtained from space-time correlations does not obey a simple power law either. Hence it is crucial in the non-equilibrium aging scaling regime to plot the data for associated two-time autocorrelations not simply as functions of the time ratio t/s, but instead against $L(t)/L(s)$ in order to attain convincing data collapse [28, 31]. It is tempting to try a similar approach in the considerably more complex disordered vortex matter system under investigation here, for which previous Monte Carlo as well as Langevin molecular dynamics simulations have yielded very complicated behavior in their non-equilibrium relaxation kinetics [20, 21, 22]. We have indeed checked if data scaling collapse ensues if we plot our Monte Carlo aging data for two-time correlation functions of Ref. [20] versus $\xi(t)/\xi(s)$ with the characteristic length scales measured in this current work. However, the results turned out unsatisfactory; in fact, the various competing energy contributions to the Hamiltonian (1) induce intricate crossovers between distinct relaxation time regimes, which however differ depending on the observable under consideration. Hence there does not exist a single characteristic and dominant length scale that governs all physical quantities of this complex system, which renders any truly simple aging scaling picture obsolete.

Acknowledgments

[1] Blatter G, Feigel'man M V, Geshkenbein V B, Larkin A I, and Vinokur V M, 1994 *Rev. Mod. Phys.* **66** 1125
[2] Nattermann T and Scheidl S, 2000 *Adv. Phys.* **49** 607
[3] Fisher M P A, 1989 **Phys. Rev. Lett. 62** 1415
[4] Feigel'man M V, Geshkenbein V B, Larkin A I, and Vinokur V M, 1989 *Phys. Rev. Lett.* **63** 2303
[5] Nattermann T, 1990 *Phys. Rev. Lett.* **64** 2454
[6] Fisher D S, Fisher M P A, and Huse D A, 1991 *Phys. Rev. B* **43** 130
[7] Giamarchi T and Le Doussal P, 1994 *Phys. Rev. Lett.* **72** 1530
[8] Giamarchi T and Le Doussal P, 1995 *Phys. Rev. B* **52** 1242
[9] Kierfeld J, Nattermann T, and Hwa T, 1997 *Phys. Rev. B* **55** 626
[10] Fisher D S, 1997 *Phys. Rev. Lett.* **78** 1964
[11] Giamarchi T and Le Doussal P, 1997 *Phys. Rev. B* **55** 6577
[12] Nelson D R and Vinokur V M, 1992 *Phys. Rev. Lett.* **68** 2398
[13] Lyuksyutov I F, 1992 *Europhys. Lett.* **200** 273
[14] Nelson D R and Vinokur V M, 1993 *Phys. Rev. B* **48** 13060
[15] Täuber U C and Nelson D R, 1997 *Phys. Rep.* **289** 157; Täuber U C and Nelson D R, 1998 *Phys. Rep.* **296** 337
[16] Bustingorry S, Cugliandolo L F, and Domínguez D, 2006 *Phys. Rev. Lett.* **96** 027001
[17] Bustingorry S, Cugliandolo L F, and Domínguez D, 2007 *Phys. Rev. B* **75** 024506
[18] Bustingorry S, Cugliandolo L F, and Iguain J L, 2007 *J. Stat. Mech.* P09008
[19] Iguain J L, Bustingorry S, Kolton A B, and Cugliandolo L F, 2009 *Phys. Rev. B* **80** 094201
[20] Pleimling M and Täuber U C, 2011 *Phys. Rev. B* **84** 174509
[21] Dobramysl U, Assi H, Pleimling M, and Täuber U C, 2013 *Eur. Phys. J. B* **86** 228
[22] Assi H, Chaturvedi H, Dobramysl U, Pleimling M, and Täuber U C, arXiv:1505.06240.
[23] Das J, Bullard T J, and Täuber U C, 2003 *Physica A* **318** 48
[24] Bullard T J, Das J, Daquila G L, and Täuber U C, 2008 *Eur. Phys. J. B* **65** 469
[25] Kisker J, Santen L, Schreckenberg M, and Rieger H, 1996 *Phys. Rev. B* **53** 6418
[26] Franz S and Parisi G, 2000 *J. Phys.: Condens. Matter* **12** 6335
[27] Corberi F, Cugliandolo L F, and Yoshina H, in *Dynamical Heterogeneities in Glasses, Colloids, and Granular Media*, edited by Berthier L and Biroli G, p. 370 (2011)
[28] Park H and Pleimling M, 2010 *Phys. Rev. B* **82** 144406
[29] Corberi F, Lippiello E, Mukherjee A, Puri S, and Zannetti M, 2011 *J. Stat. Mech.* P03016
[30] Corberi F, Lippiello E, Mukherjee A, Puri S, and Zannetti M, 2012 *Phys. Rev. E* **85** 021141
[31] Park H and Pleimling M, 2012 *Eur. Phys. J. B* **55** 300
[32] Corberi F, Lippiello E, Mukherjee A, Puri S, and Zannetti M, 2013 **Phys. Rev. E 88** 042129
[33] Mandal P K and Sinha S, 2014 *Phys. Rev. E* **89** 042144
[34] Schehr G and Le Doussal P, 2004 *Phys. Rev. Lett.* **93** 217201
[35] Schehr G and Rieger H, 2005 *Phys. Rev. B* **71** 184202
[36] Belleti F et al., 2009 *J. Stat. Phys.* **135** 1121
[37] Ray D, Olson Reichhardt C J, Janko B, and Reichhardt C, 2013 *Phys. Rev. Lett.* **110** 267001
[38] Ray D, Reichhardt C, Olson Reichhardt C J, and Janko B, 2014 *Physica C* **503** 123
[39] Ray D, Reichhardt C, and Olson Reichhardt C J, 2014 *Phys. Rev. B* **90** 094502
[40] Civale L, Marwick A D, Worthington T K, Kirk M A, Thompson J R, Krusin-Elbaum L, Sun Y, Clem J R, and Holtzberg F, 1991 *Phys. Rev. Lett.* **67** 648